

# Effects of serum protein on ionic exchange between culture medium and microporous hydroxyapatite and silicate-substituted hydroxyapatite

Katharina Guth · Charlie Campion ·  
Tom Buckland · Karin A. Hing

Received: 20 April 2011 / Accepted: 28 July 2011 / Published online: 23 August 2011  
© Springer Science+Business Media, LLC 2011

**Abstract** It has been proposed that one of the underlying mechanisms contributing to the bioactivity of osteoinductive or osteoconductive calcium phosphates involves the rapid dissolution and net release of calcium and phosphate ions from the matrix as alternatively a precursor to subsequent re-precipitation of a bone-like apatite at the surface and/or to facilitate ion exchange in biochemical processes. In order to confirm and evaluate ion release from sintered hydroxyapatite (HA) and to examine the effect of silicate substitution into the HA lattice on ion exchange under physiological conditions we monitored  $\text{Ca}^{2+}$ ,  $\text{PO}_4^{3-}$  and  $\text{SiO}_4^{4-}$  levels in Earl's minimum essential medium (E-MEM) in the absence (serum-free medium, SFM) or presence (complete medium, C-MEM) of foetal calf serum (FCM), with both microporous HA or 2.6 wt% silicate-substituted HA (SA) sintered discs under both static and semi-dynamic (SD) conditions for up to 28 days. In SFM, variation in  $\text{Ca}^{2+}$  ion concentration was not observed with either disc chemistry or culture conditions. In C-MEM,  $\text{Ca}^{2+}$  ions were released from SA under static and SD conditions whereas with HA  $\text{Ca}^{2+}$  was depleted under SD conditions.  $\text{PO}_4^{3-}$  depletion occurred in all cases, although it was greater in C-MEM, particularly under SD conditions.  $\text{SiO}_4^{4-}$  release occurred from SA irrespective of medium or culture conditions but a sustained release only occurred in C-MEM under SD conditions. In conclusion we showed that under physiological conditions the reservoir of

exchangeable ions in both HA and SA in the absence of serum proteins is limited, but that the presence of serum proteins facilitated greater ionic exchange, particularly with SA. These observations support the hypothesis that silicate substitution into the HA lattice facilitates a number of ionic interactions between the material and the surrounding physiological environment, including but not limited to silicate ion release, which may play a key role in determining the overall bioactivity and osteoconductivity of the material. However, significant net release of  $\text{Ca}^{2+}$  and  $\text{PO}_4^{3-}$  was not observed, thus rapid or significant net dissolution of the material is not necessarily a prerequisite for bioactivity in these materials.

## 1 Introduction

Hydroxyapatite (HA) has been used extensively as a bone grafting material in hard tissue implants for over 30 years [1]. Its clinical utility is supported by a number of beneficial properties such as its biocompatibility and ability to encourage direct formation of bone on its surface (osteoconductivity) and to bond chemically to bone (bioactivity) [2, 3]. The reactivity of HA with existing bone in terms of dissolution, precipitation and ion exchange is however lower than that of natural bone mineral, bi-phasic calcium-phosphates and other synthetic materials such as bioactive glasses and selected glass ceramics [4–8]. Thus, the intrinsic osteoconductivity of HA is perceived, by some, to be overshadowed by the lack of reactivity as assessed by methods such as simulated body fluid (SBF) or Tris buffer testing. Under these conditions, reactivity is considered to be predictive of both bioactivity and the capacity of the graft material to undergo complete or significant remodelling in the longer term [4, 9, 10].

K. Guth · C. Campion · K. A. Hing (✉)  
Department of Materials and Interdisciplinary Research Centre  
in Biomedical Materials, School of Engineering and Materials,  
Queen Mary University of London, London E1 4NS, UK  
e-mail: k.a.hing@qmul.ac.uk

C. Campion · T. Buckland  
ApaTech Ltd, 370 Centennial Park, Elstree, Herts WD6 3TJ, UK

Although HA is a hydrated calcium phosphate ( $\text{Ca}_{10}(\text{PO}_4)_6(\text{OH})_2$ ) with a crystallographic structure similar to that of bone mineral, it differs in that it lacks certain trace ionic substitutions [11]. Means of improving the bioactivity and osteoconductivity of HA-based bone grafting materials to promote more rapid healing have been investigated. Efforts have focussed on developing materials that mimic more closely the composition of bone (than pure HA) in terms of their physiochemical properties. Silicon has long been known to play an important role in bone formation and health [12]. HA-based materials incorporating various levels of silicate within their chemical structure have been assessed in various experimental models [13–15]. Inclusion of 0.8% by weight silicon as 2.6% by weight silicate within the calcium phosphate structure appears to enhance the apposition rate of immature woven bone and the remodelling process that generates mature lamellar bone. However, there is a clear ‘dose dependency’ with regard to the level of silicate substitution, where silicon levels of 1.5% by weight were not associated with further improvements and silicon contents of 0.2 and 0.4% by weight were associated with a reduction in the volume of bone formation as compared with stoichiometric HA [14, 15]. An additional strategy has involved investigation of both the macro- and microstructural features of a graft on the rate and volume of bone regeneration, where the inclusion of interconnected microporosity (also known as strut porosity) with a pore size of 1–50  $\mu\text{m}$ , reflecting the osteocyte lacunae and canaliculi network within bone, seems key to attaining optimal bioactivity [16, 17]. Thus by incorporating both physiologically relevant levels of silicate within the chemical structure and an interconnected microporosity silicate-substituted HA graft materials (SA) have been designed to share some of the chemical and microstructural characteristics of bone [16, 17].

It has been proposed that one of the underlying mechanisms responsible for the bioactivity of HA involves the dissolution of calcium and phosphate ions from the HA matrix [9], where dissolution leads to increases in calcium and phosphate ion concentration in the spaces between existing bone and the implanted graft which may then drive more rapid bone apposition at the graft surface [10]. It has thus been postulated that synthetic graft materials with chemical and physical properties that hasten the process of dissolution could potentially promote faster apatite formation and healing at the site of graft implantation [4, 6, 9]. Determination of whether silicate substitution significantly enhances HA dissolution rate is therefore key to understanding its mechanisms of action, in tandem with consideration of whether enhanced bone healing is additionally related to release of local bioavailable silicate ions which may act on bone cell metabolism and whether physio-

chemical modulation of protein speciation and conformation at the SA surface may promote bone cell adhesion and differentiation [18–20]. A number of studies have been performed to investigate the variation in dissolution rate of HA and SA [21–23], however, there are few studies that analyse the release of calcium, phosphate and silicate from substrates in physiologically relevant media with and without the presence of serum proteins [24]. Moreover, studies have rarely focused on the chemical composition of the material alone as experiments have only infrequently controlled for the microstructural properties and chemistry of the samples. Furthermore, experiments have rarely been conducted on materials that have an interconnected strut porosity similar to that used in clinical applications.

Thus, there remains a lack of understanding on how relative levels of ionic exchange from graft materials of differing chemical composition affect the bioactivity of HA-based bone graft substitutes. The question also arises as to what role ionic dissolution plays in the previously reported superior bioactivity of SA compared with HA in terms of species other than silicate. In the present study, we investigated the exchange of calcium, phosphate and silicate ions with microporous SA (0.8 wt% Si) and HA discs in tissue culture medium in the absence and presence of serum proteins under static and semi-dynamic (SD) conditions in order to identify any significant variation in ion exchange profile between HA and SA as well as sensitivity to the presence of serum proteins.

## 2 Materials and methods

Unless otherwise stated, all reagents were supplied by Sigma Aldrich Company (Dorset, UK).

### 2.1 Media preparation

Complete medium (C-MEM) was prepared by supplementing Earl’s minimum essential medium (E-MEM) (500 ml) with heat inactivated foetal calf serum (FCS) (50 ml), 0.9% L-glutamate (5 ml) and 0.9% penicillin–streptomycin (5 ml). Serum-free medium (SFM) was prepared in the same way as C-MEM but without the addition of FCS.

### 2.2 Media stability

To monitor the stability of the tissue culture media used in the study, samples of C-MEM and SFM were incubated in triplicate under cell culture conditions: 37°C, 5% carbon dioxide and 95% air humidity for up to 28 days. Specimens were collected on days 1, 3, 7, 10, 14, 21 and 28 and frozen at  $-20^\circ\text{C}$  for analysis of calcium, phosphate and silicate ion concentration.

### 2.3 Sample preparation

Both phase pure stoichiometric HA and 2.6 wt% silicate ( $\text{SiO}_4^{4-}$ ) substituted SA powder (i.e. containing 0.8 wt% Si) were synthesised using an aqueous precipitation method as described previously [25]. Microporous SA and HA discs with matched pore structures, similar to the strut porosity (i.e., the fraction of porosity within the scaffold struts [16] found in some bone graft substitutes [26]) were prepared by casting aqueous slurries of HA and SA powder into polytetrafluoroethylene moulds (19 mm in diameter and 8 mm deep). Castings were allowed to air dry at room temperature prior to sintering at either 1,250°C (HA) or 1,300°C (SA) (Carbolite RF 1600, Carbolite, UK) for 2 h. These conditions having been optimised to produced HA and SA microporous discs with matched microstructural characteristics [18]. Discs were sterilised in a dry oven at 160°C for 2 h prior to immersion in media.

Microporous (1 g) discs (HA or SA;  $\times 3$ ) were immersed in C-MEM or SFM (1 ml) in 24-well plates and incubated under two different sets of conditions, static and SD. Under static conditions samples were incubated under standard tissue culture conditions without agitation for periods of 1, 3, 7, 10, 14, 21 and 28 days and sample medium was not changed during the incubation period. Under SD conditions samples were also incubated under standard tissue culture conditions but the incubating media (1 ml) was collected and the media replenished with fresh SFM or C-MEM on days 1, 3, 7, 10, 14, 17, 21 and 28. All sample aliquots were stored at  $-20^\circ\text{C}$  until further analysis. Control samples consisted of the appropriate tissue culture medium incubated alone and processed in the same way as samples containing HA and SA.

### 2.4 Calcium assay

Calcium ion ( $\text{Ca}^{2+}$ ) concentration was determined using a QuantiChrom™ calcium assay kit (BioAssay Systems, Hayward, USA), in accordance with the manufacturer's instructions. A standard calibration curve for  $\text{Ca}^{2+}$  was prepared from a stock calcium solution in order to provide eight different concentrations ranging from 0 to 5 mM. The calcium assay reagent provided with the kit consisted of equal volumes of assay Reagent 'A' and assay Reagent 'B' (exact composition not available). For the assay, 5  $\mu\text{l}$  of the calibration standard or sample ( $n = 3$ ) and 200  $\mu\text{l}$  assay reagent was added to a 96-well plate. The 96-well plate was left for 5 min at room temperature and then read at 590 nm using a MultiScan Ascent™ plate reader and its associated software (Labsystems, UK).

### 2.5 Phosphate assay

Phosphate ion ( $\text{PO}_4^{3-}$ ) concentration was determined using a modified form of a previously published assay [27], that was not significantly affected by the presence of the pH indicator phenol red or  $\beta$ -glycerophosphate in tissue culture medium [28]. The phosphate assay reagent was prepared by mixing 6 M sulphuric acid, deionised water, 2.5% ammonium molybdate and 10% (w/v) ascorbic acid in a 1:2:1:1 ratio. A phosphate standard calibration curve was prepared from a stock solution of 100 mM sodium phosphate dibasic dodecahydrate ( $\text{Na}_2\text{HPO}_4 \cdot 12\text{H}_2\text{O}$ ) in deionised in order to provide 16 different concentrations ranging from 0 to 9 mM. For the assay, 20  $\mu\text{l}$  standard solution or sample ( $n = 3$ ) was added to a 96-well plate and to this, 80  $\mu\text{l}$  deionised water and 100  $\mu\text{l}$  of the phosphate assay reagent was added. The plates were shaken for 10 s, sealed and incubated at 37°C for 2 h. After 2 h, the plates were allowed to return to room temperature and the absorbance was read at 810 nm using a MultiScan Ascent™ plate reader and its associated software (Labsystems, UK).

### 2.6 Silicate assay

The assay was a modified form of a previously published assay [29]. The silicate assay Reagent 'A' was prepared by mixing 4.5 M sulphuric acid and 0.6 M ammonium molybdate in a 1:1 ratio. The silicate assay Reagent 'B' was prepared by mixing 10% (w/v) oxalic acid and 3% (w/v) ascorbic acid in a 1:1 ratio. To obtain a 1.7 mM stock solution, 10  $\mu\text{l}$  sodium silicate solution (BDH Laboratory supplies, Poole, UK) was mixed with 990  $\mu\text{l}$  distilled water. This stock solution (290  $\mu\text{l}$ ) was added to C-MEM or SFM (10 ml), from which a serial dilution of eight points ranging from 0 to 125  $\mu\text{g ml}^{-1}$  was obtained. For the assay, 100  $\mu\text{l}$  standard or sample ( $n = 3$ ) were added to a 96-well plate to which 100  $\mu\text{l}$  Reagent 'A' was added. After 1.5 h at room temperature, 60  $\mu\text{l}$  of Reagent 'B' was added and 10 min later the absorbance was read at 810 nm using a MultiScan Ascent™ plate reader and its associated software (Labsystems, UK).

### 2.7 pH analysis

The pH was measured using a calibrated pH meter (Hanna Instruments, UK), which automatically recorded both pH and temperature every 5 min. To measure pH, SFM (50 ml) pre-warmed to 37°C was incubated under cell culture conditions for 50 min to reach equilibrium. Microporous HA or SA (50 g;  $n = 5$ ) were immersed in the equilibrated SFM and pH (temperature corrected) was monitored for 2 h.

## 2.8 Statistical analysis

Values of variance ( $R^2$ ) were determined for the calibration curves of the calcium, phosphate and silicate assays. Calibration curves were used to determine ionic concentrations only when  $R^2$  values were greater than 0.99. Mean  $\pm$  standard deviation values were determined for calcium, phosphate and silicate ion concentrations for each of the incubation systems investigated. Differences between control samples and medium collected after exposure to either HA or SA discs were assessed statistically using a one-way analysis of variance (ANOVA) and evaluated using Dunnett's post-hoc testing. Differences between HA and SA sample data were assessed statistically using the Wilcoxon–Mann–Whitney tests. All statistical tests were run using KaleidaGraph statistical software (v 4.0, Synergy Software, USA) where values of  $\alpha$  of less than 0.05 were taken as representing statistical significance.

## 3 Results

### 3.1 Medium stability

In the absence of discs,  $\text{Ca}^{2+}$  and  $\text{PO}_4^{3-}$  ion concentrations in both the SFM and C-MEM did not vary over the 28-day incubation period under either static or SD conditions. The addition of FCS had no clear effect on the  $\text{Ca}^{2+}$  concentration of either medium (SFM =  $79 \pm 12 \mu\text{g ml}^{-1}$ , C-MEM =  $81 \pm 11 \mu\text{g ml}^{-1}$ ) but markedly increased  $\text{PO}_4^{3-}$  concentration (SFM =  $99 \pm 17 \mu\text{g ml}^{-1}$ , C-MEM =  $155 \pm 8 \mu\text{g ml}^{-1}$ ;  $P < 0.0001$ ; Table 1). There was a discrepancy between the  $\text{Ca}^{2+}$  and  $\text{PO}_4^{3-}$  ion concentrations cited by the manufacturer for E-MEM (Table 1) and the levels measured in SFM during the study;  $\text{Ca}^{2+}$  concentration being significantly lower ( $P < 0.05$ ) and  $\text{PO}_4^{3-}$  concentration moderately higher than specified.

### 3.2 Calcium ion concentration

The mean  $\text{Ca}^{2+}$  concentration remained relatively constant with minimal depletion or release detected in SFM in the

presence of either SA or HA under static conditions over the 28-day time period (Fig. 1a). A significant depletion of  $\text{Ca}^{2+}$  was detected in SFM in the presence of SA at day 3 ( $P < 0.05$ ) and at day 14 ( $P < 0.05$ ) in the presence of HA. Under SD conditions there was a net depletion in the mean  $\text{Ca}^{2+}$  concentration of SFM in the presence of both HA and SA over the 28-day time period (Fig. 1b). Under these conditions depletion of  $\text{Ca}^{2+}$  in SFM in the presence of SA was statistically significant on day 1 ( $P < 0.005$ ) and days 3, 10, 14 and 28 (all  $P < 0.05$ ). In the presence of HA, significant differences were observed on days 3, 10, 14 and 28 (all  $P < 0.05$ ). On day 1, the level of  $\text{Ca}^{2+}$  depletion was significantly greater in the presence of SA than HA ( $P < 0.05$ ).

Under static conditions the  $\text{Ca}^{2+}$  concentration in C-MEM in the presence of HA remained relatively constant over the 28-day incubation period (Fig. 1c) and did not vary significantly from that detected in control C-MEM samples. In contrast, the  $\text{Ca}^{2+}$  concentration in C-MEM in the presence of SA under static conditions demonstrated a statistically significant increase on day 3 ( $P < 0.05$ ), day 7 ( $P < 0.05$ ), day 10 ( $P < 0.0001$ ), day 14 ( $P < 0.001$ ), day 21 ( $P < 0.0001$ ) and day 28 ( $P < 0.0001$ ; Fig. 1c). The  $\text{Ca}^{2+}$  concentrations in C-MEM were greater in the presence of SA than HA, with statistically significant differences observed on day 10 ( $P < 0.05$ ), day 14 ( $P < 0.005$ ), day 21 ( $P < 0.05$ ) and day 28 ( $P < 0.005$ ). Under SD conditions,  $\text{Ca}^{2+}$  concentrations in C-MEM depleted in the presence of HA, with statistically significant differences emerging on day 3 ( $P < 0.005$ ) that continued until day 28 [day 10 ( $P < 0.05$ ), day 14 ( $P < 0.001$ ), day 21 ( $P < 0.05$ ) and day 28 ( $P < 0.001$ ; Fig. 1d)]. Concentration of  $\text{Ca}^{2+}$  in C-MEM in the presence of SA showed some variability over 28 days of the study. Calcium ion concentrations were significantly depleted at day 1 ( $P < 0.05$ ), but showed no marked variation from day 3 to day 28 (Fig. 1d). From day 10 to day 28,  $\text{Ca}^{2+}$  concentrations in C-MEM were significantly greater ( $P < 0.05$  on days 10–21;  $P < 0.005$  on day 28) in the presence of SA than HA (Fig. 1d).

### 3.3 Phosphate ion concentration

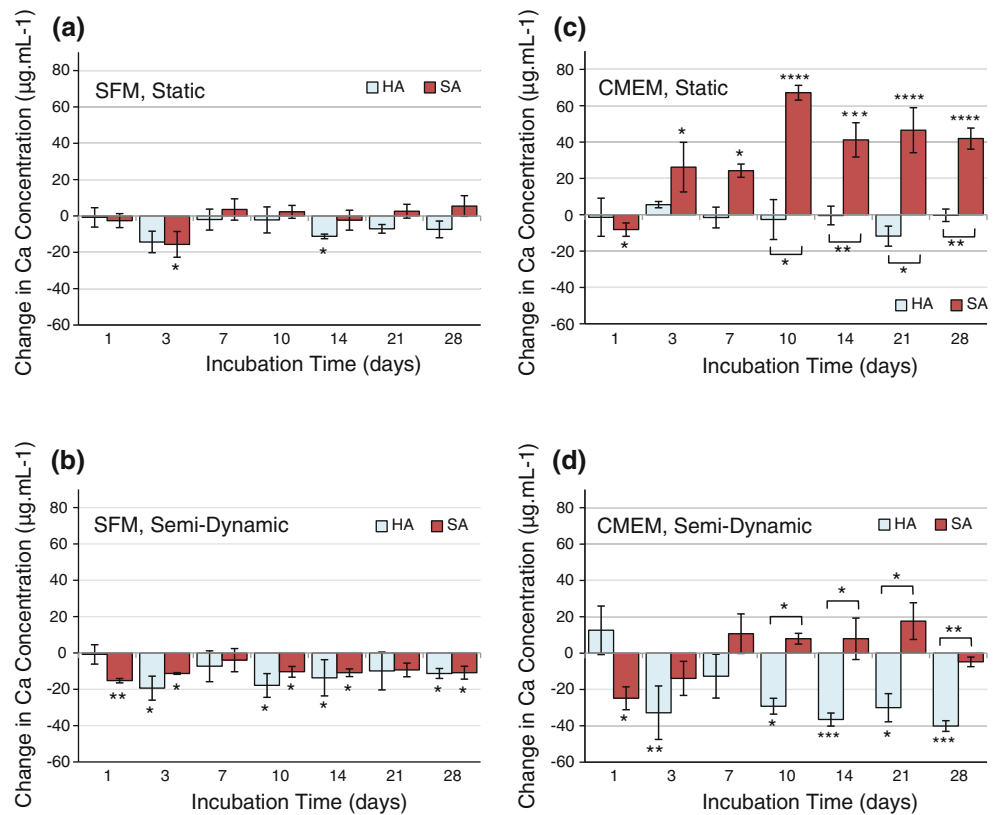
Under static conditions, the phosphate ion concentration of SFM was significantly depleted in the presence of both HA and SA ( $P < 0.0001$ ) across all time points (Fig. 2a). The degree of  $\text{PO}_4^{3-}$  depletion from SFM was initially less pronounced in the presence of SA resulting in statistically significant higher phosphate ion concentrations on days 1–7 ( $P < 0.0001$ ) and days 10–14 ( $P < 0.001$ ) compared with values of SFM in the presence of HA. On day 21 and day 28,  $\text{PO}_4^{3-}$  depletion of SFM was statistically similar in the presence of either SA or HA. Under SD conditions,  $\text{PO}_4^{3-}$  depletion was less pronounced in SFM in the

**Table 1** Absolute calcium and phosphate ion concentrations of E-MEM, C-MEM and SFM

	Data provided for E-MEM (mean) <sup>a</sup>	C-MEM analysed mean ( $\pm$ SD)	SFM analysed mean ( $\pm$ SD)
Calcium ions ( $\mu\text{g ml}^{-1}$ )	96	$81 \pm 11$	$79 \pm 12$
Phosphate ions ( $\mu\text{g ml}^{-1}$ )	97	$155 \pm 8$	$99 \pm 17$

<sup>a</sup> Data provided by manufacturer

**Fig. 1** Mean change in calcium ion concentrations of HA and SA incubated in **a** serum free medium under static conditions, **b** serum free medium under SD conditions, **c** complete medium under static conditions, **d** complete medium under SD conditions for up to 28 days (variation in significance level as compared to basal levels and between HA and SA denoted by \* $P < 0.05$ ; \*\* $P < 0.005$ ; \*\*\* $P < 0.001$ ; \*\*\*\* $P < 0.0001$ ; basal  $\text{Ca}^{2+}$  concentration of SFM =  $79 \pm 12 \mu\text{g ml}^{-1}$ ; basal  $\text{Ca}^{2+}$  concentration of C-MEM =  $81 \pm 11 \mu\text{g ml}^{-1}$ ; error bars standard error)



presence of both HA and SA compared with static conditions. The degree of ion depletion in the presence of SA was lower compared with the SFM control with statistically significant differences observed at all time points apart from day 14 and day 28 (Fig. 2b). Concentration of  $\text{PO}_4^{3-}$  in the presence of HA was lower than the SFM control with statistically significant differences in ion depletion observed at all time points ( $P < 0.0001$ ; Fig. 2b). Under SD conditions,  $\text{PO}_4^{3-}$  depletion of SFM was statistically significantly greater in the presence of HA compared with SA on day 3 ( $P < 0.001$ ), day 7 and day 10 ( $P < 0.05$ ), day 14 ( $P < 0.005$ ) and day 21 and day 28 ( $P < 0.001$ ; Fig. 2b).

Under both static and SD conditions,  $\text{PO}_4^{3-}$  depletion of C-MEM in the presence of both HA and SA was greater compared with C-MEM control ( $1.6 \pm 0.1 \text{ mM}$ ) at all time points ( $P < 0.0001$ ) (Fig. 2c, d). Under static conditions, over the 28-day time period, the mean  $\text{PO}_4^{3-}$  depletion from C-MEM in the presence of HA was  $1.4 \pm 0.1 \text{ mM}$  compared with  $1.1 \pm 0.1 \text{ mM}$  in the presence of SA, these differences achieved statistical significance ( $P < 0.005$ ). Under SD conditions, phosphate ion concentration in C-MEM in the presence of HA was initially similar to static conditions ( $1.4 \pm 0.1 \text{ mM}$ ), however, over the incubation period, ion concentration decreased and a mean  $\text{PO}_4^{3-}$  concentration of  $0.96 \text{ mM}$  was recorded on day 28. Although there was a degree of variation in the level of  $\text{PO}_4^{3-}$  depletion from

C-MEM exposed to SA over the 28-day period, values tended to fluctuate around  $1.0 \pm 0.1 \text{ mM}$ . The mean  $\text{PO}_4^{3-}$  depletion in C-MEM under SD conditions was statistically greater in the presence of HA than SA on days 1–14 ( $P < 0.005$ ; Fig. 2d). On day 28, however,  $\text{PO}_4^{3-}$  depletion from C-MEM in the presence of SA was significantly greater than HA ( $P < 0.05$ ; Fig. 2d).

### 3.4 Silicate ion concentration

Silicate ions ( $\text{SiO}_4^{4-}$ ) were not detected in SFM or C-MEM, alone or in the presence of HA at any time point over 28 days under static or SD conditions. For SFM in the presence of SA under static conditions,  $\text{SiO}_4^{4-}$  concentrations increased upon incubation, peaking on day 14 ( $0.25 \pm 0.02 \text{ mM}$ ) and then fluctuated until day 28 (Fig. 3a). Under SD conditions, SFM  $\text{SiO}_4^{4-}$  concentrations were greatest during the initial 7 days, peaking at day 1 ( $0.25 \pm 0.02 \text{ mM}$ ). Only traces of  $\text{SiO}_4^{4-}$  were detected from day 10 onwards (Fig. 3b).

Concentrations of  $\text{SiO}_4^{4-}$  for SA incubated in C-MEM under static conditions gradually increased, peaking at day 10 ( $2.0 \pm 0.01 \text{ mM}$ ). The release of  $\text{SiO}_4^{4-}$  in C-MEM decreased on day 14 ( $1.6 \pm 0.07 \text{ mM}$ ) and then did not vary significantly with time (Fig. 3c). Under SD conditions,  $\text{SiO}_4^{4-}$  concentration in C-MEM increased steadily to day 7 (Fig. 3d) then fluctuated until day 28.

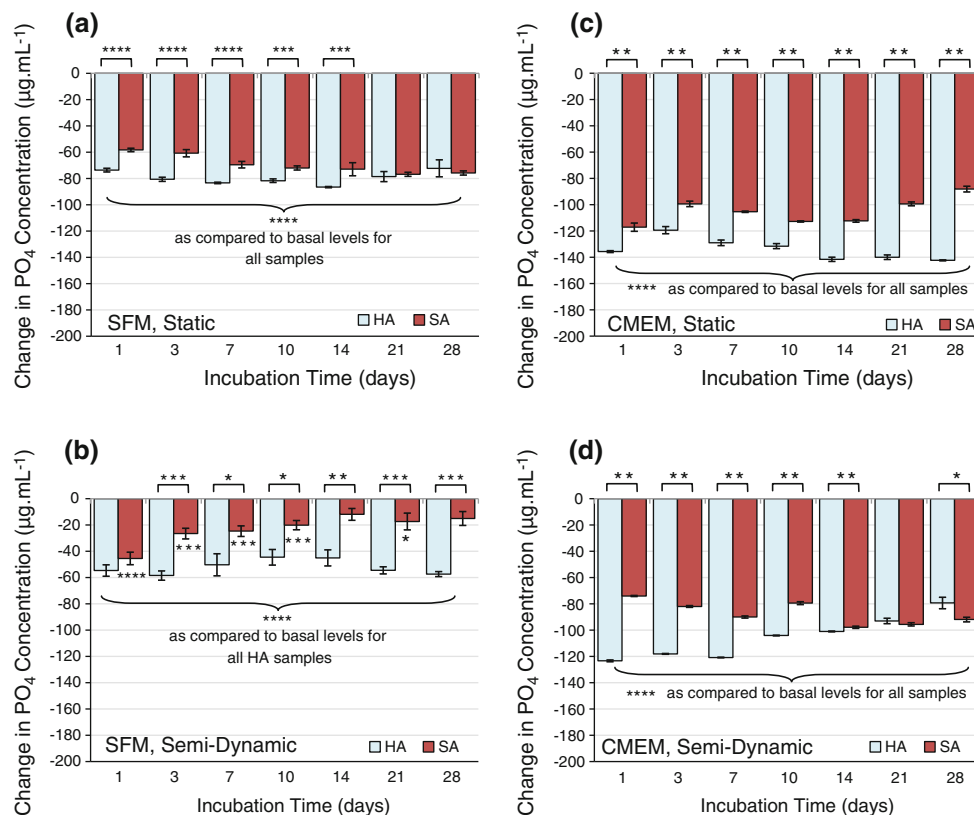


**Fig. 2** Mean phosphate ion concentrations of HA and SA incubated in **a** serum free medium under static conditions, **b** serum free medium under SD conditions, **c** complete medium under static conditions, **d** complete medium under SD conditions for up to 28 days (variation in significance level as compared to basal levels and between HA

and SA denoted by \* $P < 0.05$ ; \*\* $P < 0.005$ ; \*\*\* $P < 0.001$ ; \*\*\*\* $P < 0.0001$ ; basal  $\text{PO}_4^{3-}$  concentration of SFM =  $99 \pm 17 \mu\text{g ml}^{-1}$ ; basal  $\text{PO}_4^{3-}$  concentration of C-MEM =  $155 \pm 8 \mu\text{g ml}^{-1}$ ; error bars standard error)

### 3.5 pH variations in serum free medium

There was no variation in the pH of pre-warmed SFM alone under cell culture conditions over 50 min (Fig. 4a). The pH of SFM in the presence of HA was also unchanged (mean pH of  $7.70 \pm 0.01$ ) over a period of 150 min (Fig. 4b). However, in the presence of SA, the pH of SFM increased with time from 7.70 to 9.20 over 150 min and by 20 min, the pH of SFM in the presence of SA was significantly higher than that of SFM in the presence of HA ( $P < 0.01$ ; Fig. 4b).

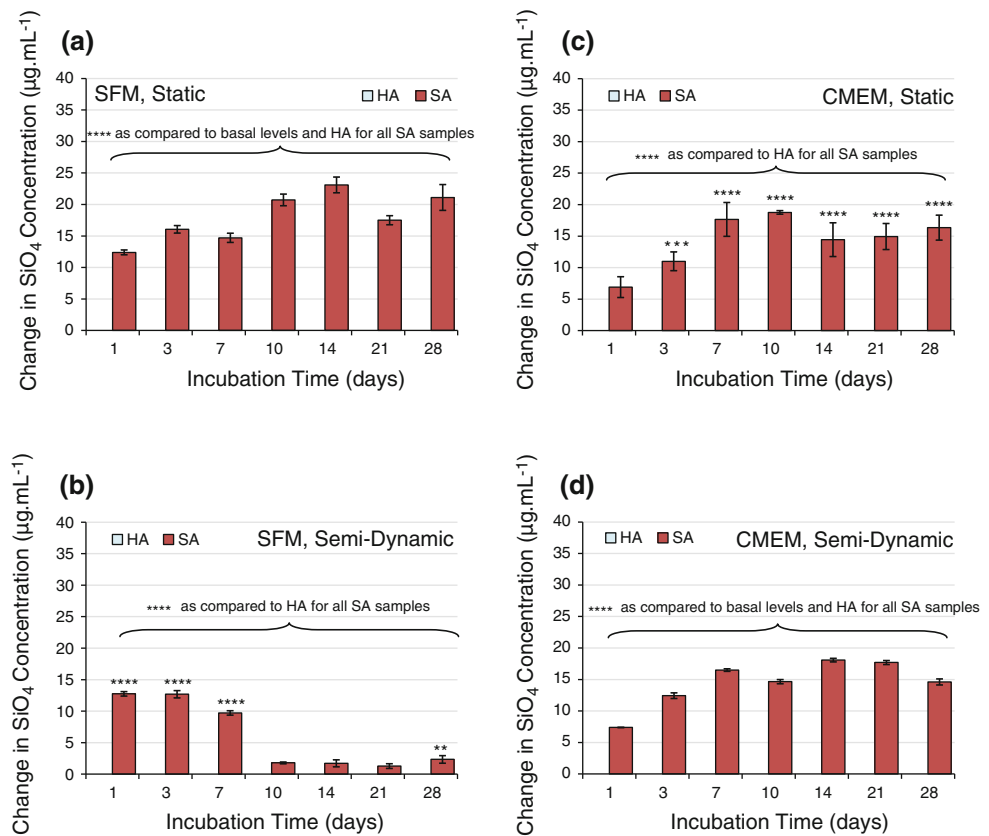
## 4 Discussion

It is widely accepted that SA has beneficial biological properties over stoichiometric HA and that this may be due to the effect of silicate ion release from these materials on bone metabolism [30]. A recent review of data in the scientific literature suggests that experimental data demonstrating the release of  $\text{SiO}_4^{4-}$  ions at therapeutic concentrations is required to support this assumption and

that there is no study clearly linking the improved biological performance of silicate-substituted calcium phosphates to  $\text{SiO}_4^{4-}$  release alone [24], although indirect cell culture studies have identified that osteoblast like cell metabolism is stimulated when incubated in the presence of SA discs so removing surface texture and surface physiochemistry as confounding variables [31]. The aim of this study was to monitor the exchange of calcium, phosphate and silicate ions between microporous SA and HA discs in SFM and C-MEM under static and SD conditions so as to determine whether calcium and phosphate ion release profiles were significantly altered with silicate substitution as well as to identify any sensitivity to the presence of serum proteins. Review of our data clearly demonstrates that there are differences in the patterns of ion exchange between culture medium and microporous apatite that are related to test conditions (static vs. SD) and the presence of serum proteins that, for  $\text{Ca}^{2+}$  and  $\text{PO}_4^{3-}$  ion exchange are at least as significant as the nature of the disc chemistry.

In a static serum free environment over the 28 day time period of the study, silicate substitution did not appear to have a significant effect on apatite stability. There was no

**Fig. 3** Mean silicate ion concentrations of SA incubated in **a** serum free medium under static conditions, **b** serum free medium under SD conditions, **c** complete medium under static conditions, **d** complete medium under SD conditions for up to 28 days (variation in significance level as compared to basal levels and between HA and SA denoted by  $**P < 0.005$ ;  $***P < 0.001$ ;  $****P < 0.0001$ ; Basal  $\text{SiO}_4^{4-}$  concentration of SFM =  $0 \mu\text{g ml}^{-1}$ ; basal  $\text{SiO}_4^{4-}$  concentration of C-MEM =  $0 \mu\text{g ml}^{-1}$ ; error bars standard error)



net change or variation in  $\text{Ca}^{2+}$  concentration in SFM with time, both the apatite surfaces were found to adsorb  $\text{PO}_4^{3-}$  ions and although this level of adsorption was initially greater on HA, by 28 days  $\text{PO}_4^{3-}$  depletion levels were similar. These observations agree with previous findings suggesting that in the presence of physiological phosphate concentrations there is a significant driving force for protonated  $\text{PO}_4^{3-}$  ions to dominate at apatite surfaces to facilitate charge balance and to maintain surface neutrality [32]. Measurement of pH demonstrated that in the presence of SA, the pH of SFM increased to pH 9 in the first 2 h of incubation, whereas the pH remained unchanged in the presence of HA, presumably as a result of the release of silicate ions, and perhaps also reflecting the fact that the point of zero charge for SA is pH 8.5 compared with pH 7.3 for HA [33]. The only significant difference between the behaviour of HA and SA in static SFM was in the release of  $\text{SiO}_4^{4-}$  which attained a concentration of  $12 \mu\text{g ml}^{-1}$  at day 1 and then gradually increased to reach a plateau concentration of around  $20 \mu\text{g ml}^{-1}$  from 10 to 28 days, suggesting that minimal  $\text{SiO}_4^{4-}$  was released after 10 days.

Under SD conditions, where the media was periodically replaced, the restricted nature of the release of  $\text{SiO}_4^{4-}$  in SFM was more obvious, with  $\text{SiO}_4^{4-}$  levels reaching  $13 \mu\text{g ml}^{-1}$  at day 1 but dropping to  $2 \mu\text{g ml}^{-1}$  after

7 days. As with static SFM there was no variation in  $\text{Ca}^{2+}$  concentration with disc chemistry under SD conditions, with minor levels of  $\text{Ca}^{2+}$  depletion being observed. Although both apatite surfaces were found initially to adsorb  $\text{PO}_4^{3-}$  ions under SD conditions, the capacity of HA to adsorb  $\text{PO}_4^{3-}$  from refreshed SFM continued throughout the entire test period, whereas SA surfaces appeared to have reached saturation at 14 days. In conjunction with the slight  $\text{Ca}^{2+}$  depletion this could provide evidence of  $\text{Ca-PO}_4$  re-precipitation at the HA surfaces under these conditions.

Thus, in a serum-free environment, both SA and HA respond similarly to medium replenishment, with neither demonstrating significant net release of  $\text{Ca}^{2+}$  or  $\text{PO}_4^{3-}$  ions into the SFM. This finding appears to contradict those of an earlier study using high resolution transmission electron microscopy where it was reported that SA powders displayed increased dissolution at their surfaces as compared with HA powders in SBF [34]. The previous observation was thought to indicate that SA possesses a faster dissolution rate compared with that of HA in an aqueous environment, however, both the SA and HA powders were prepared by sintering at  $1,200^\circ\text{C}$ . In a previous study we determined that matched microstructural morphology was attained when HA and SA were sintered at  $1,250$  and  $1,300^\circ\text{C}$ , respectively [18], reflecting the fact that silicate

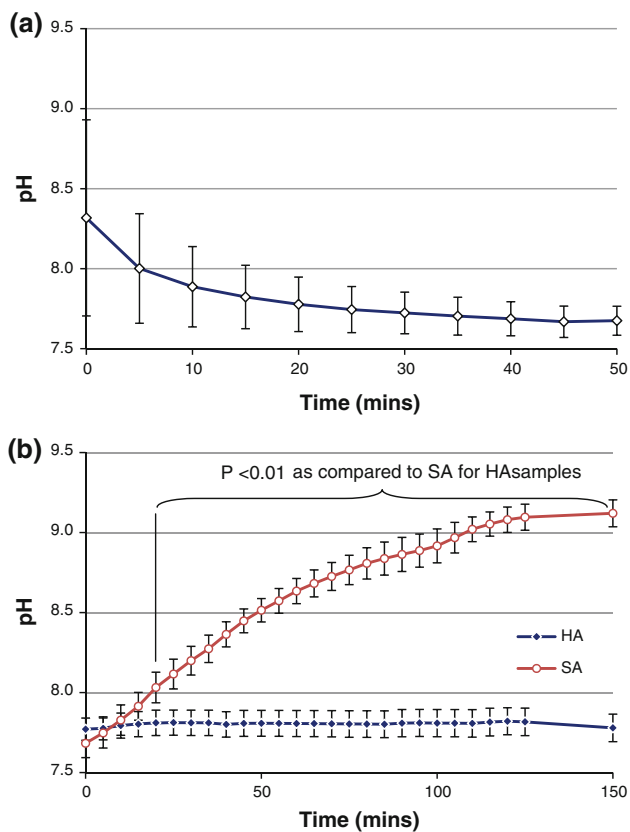


**Fig. 4** **a** Mean pH of serum free medium on introduction to cell culture conditions; **b** mean pH of pre-incubated serum free medium upon incubation with HA or SA ( $n = 5$ ) (error bars standard deviation)

addition raises the thermal stability of HA in a dose dependant manner up to the substitution limit of 1.6 wt% Si. Thus the difference in dissolution behaviour observed with powders sintered at 1,200°C may reflect the fact that the SA was relatively undersintered as compared to the HA. The results of the current study suggest that for fully sintered material in an aqueous environment devoid of protein, dissolution may be limited to a defect rich ‘surface layer’ resulting in a limited release of  $\text{SiO}_4^{4-}$  rather than demonstrating a continual release profile. It is possible that a dynamic equilibrium is established at HA and SA surfaces under the conditions of our SFM experiment, where the surface is effectively passivated by calcium-phosphate re-precipitation and/or protonated phosphate adsorption.

One obvious difference between incubation in SFM and under in vivo conditions is the presence of biological constituents such as cells and proteins. Addition of serum proteins to the incubation medium resulted in a marked change in the pattern of behaviour of SA and HA. Under static conditions a significant release of  $\text{Ca}^{2+}$  ions into C-MEM was observed from SA, whereas no net exchange was observed from HA. In contrast, under SD conditions

there was an observed depletion of  $\text{Ca}^{2+}$  ions from C-MEM in the presence of HA and fluctuating depletion and release from SA. Considering the effect of the addition of serum proteins in isolation, it was clear that their presence had more of an impact on SA than HA. With HA, the presence of serum proteins resulted in increased levels of  $\text{PO}_4^{3-}$  and  $\text{Ca}^{2+}$  ion depletion, most significantly under semi dynamic conditions. The change in the pattern of behaviour for SA in the presence of serum was far more marked, leading to net  $\text{Ca}^{2+}$  ion release under static conditions and a greater capacity for  $\text{PO}_4^{3-}$  adsorption under semi dynamic conditions over the length of the study. However, the most obvious effect was in the continual release of  $\text{SiO}_4^{4-}$  ions into the media over 28 days under SD conditions. Collectively, these observations suggest that the SA surface may be destabilised by the dynamic adsorption and desorption of serum proteins at its interface, whereas protein interactions may actually stabilise the HA surface. This could be through pH modulation of protein activity or protein affinity for the SA surface and/or direct protein interaction with the SA surface being facilitated by differences in surface charge and ionic species at the interface. Thus, observations made in a protein free environment regarding the levels of net ion exchange at which dynamic equilibria are established do not apply in the more physiologically relevant protein containing environment.

It is widely believed that one of the stages involved in the potential ability of a bioactive material to bond directly to bone is through the formation of an apatite layer. This results from the interaction of ions at the material surface and the surrounding environment [35]. In vitro, the spontaneous formation of bone-like apatite in SBF has been associated with improved graft incorporation and adapted as an indicator of bioactivity [36]. Faster formation of apatite in SBF has been reported on SA (0.4 wt%) in vitro [13] and more compellingly more extensive apatite formation has been observed on SA (0.8, 1.5 wt%) in vivo [34], as compared with phase pure HA. In the current study, the formation of an apatite layer on the surface of SA or HA microporous discs from both SFM and C-MEM would be expected to result in a net depletion of  $\text{Ca}^{2+}$  from the media assuming no net dissolution of  $\text{Ca}^{2+}$  from the discs. The release of  $\text{Ca}^{2+}$  ions in C-MEM from SA under static conditions suggests this latter assumption can not be made, however, the lack of net  $\text{Ca}^{2+}$  ion enrichment in C-MEM when under SD conditions provides evidence for moderate levels of dissolution that are in dynamic equilibrium with any apatite formation or other processes at the sintered microporous SA disc surfaces.

The degree to which an implant can form an apatite layer is influenced by various factors, including the pH of the solution it is bathed in. In this study, we observed a shift in the pH towards higher alkalinity SFM in the



presence of SA. This was most likely a result of the release of  $\text{SiO}_4^{4-}$  combined with the net negative surface charge of SA leading to adsorption of more hydrogen ions and overcoming the buffering capacity of the cell culture medium [32, 33]. Maintaining pH in the physiological range appears to be important to normal bone repair and function [37]. Under circumstances where pH is not maintained with physiological levels in vivo, cellular apoptosis, necrosis and non specific inflammatory responses have been reported [38–40]. In the clinical setting, it is not expected that such significant increases in pH would occur in proximity to SA due to the highly dynamic fluid exchange that would be expected to occur at an implantation site. However, under static conditions where a 1 g sample is immersed in 1 ml of medium, this effect would be particularly pronounced and, interestingly, it was under these conditions that a significant net release in  $\text{Ca}^{2+}$  was observed, although only in the presence of C-MEM. Several previous studies have reported on the potential for serum proteins to promote the dissolution of minerals [41–44]. Indeed some serum proteins have been implicated in the mineralisation and remodelling process where they may have the express role of inhibiting or initiating apatite growth through their interaction with  $\text{Ca}^{2+}$  ions [42–44]. Thus it is possible that our observations of limited  $\text{Ca}^{2+}$  release may be confounded by significant protein sequestering of this ion as associated with apatite formation or retardation at the disc surfaces.

Protein conformation is also known to be highly sensitive to pH. Thus, in the negatively charged environment proximal to the SA surface, it is likely that protein–ion interactions occur that facilitate surface adsorption of the hydrophobic organic molecules on the hydrophilic SA surface. The driving force for this interaction is likely to be mediated through electrostatic and conformational changes that satisfy the entropic drive to reduce molecular order in water molecules in response to the presence of hydrophobic protein ‘surfaces’. This could lead to an inability of the SA surface to develop an effective inorganic and/or organic ‘passivating’ layer resulting in the net removal of ions from the surface through a constant process of protein ion sequestering, dynamic protein exchange and ion interchange with the surrounding media.

While the presence of silicate ions in the HA lattice did not appear to directly increase the capacity for ionic dissolution (in terms of unilateral ion release) in an aqueous environment, it did lead to an increase in local pH, accelerated uptake of  $\text{PO}_4^{3-}$  and limited release of  $\text{Ca}^{2+}$  in the presence of serum proteins. This has significant implications for the effect of silicate substitution on the local micro-environment in close proximity to silicate substituted graft surfaces in vivo. Increases in local pH, silicate ion release and dynamic calcium and phosphate ion

exchange accompanying previously demonstrated changes in protein affinity at the substituted apatite interface [18, 19], will make this a very different local environment to that found at stoichiometric apatite surfaces and provides base line evidence of differences in physiochemical response which may contribute to the enhanced bioactivity and accelerated graft remodelling as observed with these materials in vivo.

Our findings suggest that within the timescales of these experiments the reservoir of ions available for exchange from both HA and SA in the absence of serum proteins is restricted and thus likely to be surface limited. However, for SA the presence of serum proteins assuages this barrier, presumably by engaging the interface in a dynamic process of protein adsorption and desorption, facilitating the potential for greater ionic exchange between the apatite surfaces and the surrounding aqueous environment. These observations support the hypothesis that silicate substitution into the HA lattice facilitates a number of ionic and proteomic interactions between the material and the surrounding physiological environment, including silicate ion release, which may play a key role in determining the overall bioactivity and osteoconductivity of the material. However, significant net release of  $\text{Ca}^{2+}$  and  $\text{PO}_4^{3-}$  was not observed thus rapid or significant net dissolution is not necessarily a prerequisite for bioactivity in these materials.

## References

1. Aoki H. Science and medical applications of hydroxyapatite. Tokyo: Takayama Press; 1991.
2. Maxian SH, Zawadsky JP, Dunn MG. Effect of Ca/P coating resorption and surgical fit on the bone/implant interface. *J Biomed Mater Res.* 1994;28:1311–9.
3. Moroni A, Caja VL, Egger EL, Trinchese L, Chao EYS. Histomorphometry of hydroxyapatite-coated and uncoated porous titanium bone implants. *Biomaterials.* 1994;15:926–30.
4. Ducheyne P, Radin S, King L. The effect of calcium-phosphate ceramic composition and structure on in vitro behaviour. I. Dissolution. *J Biomed Mater Res.* 1993;27:25–34.
5. Schepers E, Declercq M, Ducheyne P, Kempeneers R. Bioactive glass particulate material as a filler for bone lesions. *J Oral Rehabil.* 1991;18:439–52.
6. Dalculsi G, Legeros RZ, Nery E, Lynch K, Kerebel B. Transformation of biphasic calcium phosphate ceramics in vivo: ultrastructural and physicochemical characterization. *J Biomed Mater Res.* 1989;23:883–94.
7. Holand W, Vogel W, Naumann K, Gummel J. Interface reactions between machinable bioactive glass-ceramics and bone. *J Biomed Mater Res.* 1985;19:303–12.
8. Oonishi H, Hench LL, Wilson J, Sugihara F, Tsuji E, Kushitani S, Iwaki H. Comparative bone growth behavior in granules of bioceramic materials of various sizes. *J Biomed Mater Res.* 1999;44:31–43.
9. Weng J, Liu Q, Wolke JGC, Zhang X, de Groot K. Formation and characteristics of the apatite layer on plasma-sprayed

- hydroxyapatite coatings in simulated body fluids. *Biomaterials*. 1997;18:1027–35.
10. Amarah-Bouali S, Rey C, Lebugle A, Bernache D. Surface modifications of hydroxyapatite ceramics in aqueous media. *Biomaterials*. 1994;15:269–72.
  11. Driessens FCM. The mineral in bone, dentin and tooth enamel. *Bull Soc Chim Belg*. 1980;89:663–89.
  12. Jugdaohsingh R. Silicon and bone health. *J Nutr Health Aging*. 2007;11:99–110.
  13. Gibson IR, Huang J, Best SM, Bonfield W. Enhanced in vitro cell activity and surface apatite layer formation on novel silicon-substituted hydroxyapatites. *Bioceramics*. 1999;12:191–4.
  14. Hing KA, Revell PA, Smith N, Buckland T. Effect of silicon level on rate, quality and progression of bone healing within silicate-substituted porous hydroxyapatite scaffolds. *Biomaterials*. 2006;27:5014–26.
  15. Patel N, Brooks RA, Clarke MT, Lee MT, Rushton N, Gibson IR, Best SM, Bonfield W. In vivo assessment of hydroxyapatite and silicate-substituted hydroxyapatite granules using an ovine defect model. *J Mater Sci Mater Med*. 2005;16:429–40.
  16. Hing K, Annaz B, Saeed S, Revell P, Buckland T. Microporosity enhances bioactivity of synthetic bone graft substitutes. *J Mater Sci Mater Med*. 2005;16:467–75.
  17. Rouahi M, Gallet O, Champion E, Dentzer J, Hardouin P, Anselme K. Influence of hydroxyapatite microstructure on human bone cell response. *J Biomed Mater Res A*. 2006;78:222–35.
  18. Guth K, Campion C, Buckland T, Hing KA. Surface physicochemistry affects protein adsorption to stoichiometric and silicate-substituted microporous hydroxyapatites. *Adv Eng Mater*. 2010;12:B113–21.
  19. Guth K, Campion C, Buckland T, Hing KA. Effect of silicate-substitution on attachment and early development of human osteoblast-like cells seeded on microporous hydroxyapatite discs. *Adv Eng Mater*. 2010;12:B26–36.
  20. Stephansson SN, Byers BA, Garcia AJ. Enhanced expression of the osteoblastic phenotype on substrates that modulate fibronectin conformation and integrin receptor binding. *Biomaterials*. 2002;23:2527–34.
  21. Botelho CM, Lopes CA, Gibson IR, Best SM, Santos JD. Structural analysis of Si-substituted hydroxyapatite: zeta potential and X-ray photoelectron spectroscopy. *J Mater Sci Mater Med*. 2002;13:1123–7.
  22. Balas F, Perez-Pariente J, Vallet-Regi M. In vitro bioactivity of silicon-substituted hydroxyapatites. *J Biomed Mater Res A*. 2003;66:364–75.
  23. Botelho CM, Brooks RA, Spence G, McFarlane I, Lopes MA, Best SM, Santos JD, Rushton N, Bonfield W. Differentiation of mononuclear precursors into osteoclasts on the surface of Si-substituted hydroxyapatite. *J Biomed Mater Res A*. 2006;78:709–20.
  24. Bohner M. Silicon-substituted calcium phosphates—a critical view. *Biomaterials*. 2009;30:6403–6.
  25. Gibson IR, Best SM, Bonfield W. Chemical characterisation of silicon-substituted hydroxyapatite. *J Biomed Mater Res*. 1999;44:422–8.
  26. Hing K, Wilson L, Buckland T. Comparative performance of three ceramic bone graft substitutes. *Spine J*. 2007;7:475–90.
  27. Chen PS, Toribara TY, Warner H. Microdetermination of phosphorus. *Anal Chem*. 1956;28:1756–8.
  28. Grundel R. Microscopical and biochemical studies of mineralised matrix production by human bone derived cells. Thesis submitted for Doctorate of Philosophy to Department of Orthopaedic Surgery and Wolfson College, University of Oxford, Oxford; 1995. p. 328.
  29. Raggi MA, Sabbioni C, Mandrioli R, Zini Q, Varani G. Spectrophotometric determination of silicate traces in hemodialysis solutions. *J Pharm Biomed Anal*. 1999;20:335.
  30. Pietak AM, Reid JW, Stott MJ, Sayer M. Silicon substitution in the calcium phosphate bioceramics. *Biomaterials*. 2007;28:4023–32.
  31. Guth K, Buckland T, Hing KA. Silicon dissolution from microporous silicon substituted hydroxyapatite and its effect on osteoblast behaviour. *Key Eng Mater*. 2006;117:309–11.
  32. Harding IS, Rashid N, Hing KA. Surface charge and the effect of excess calcium ions on the hydroxyapatite surface. *Biomaterials*. 2005;26:6818–26.
  33. Rashid N, Harding IS, Buckland T, Hing KA. Nano-scale manipulation of silicate-substituted apatite chemistry impacts surface charge, hydrophilicity, protein adsorption and cell attachment. *Int J Nano Biomater*. 2008;1:299–319.
  34. Porter AE, Botelho CM, Lopes MA, Santos JD, Best SM, Bonfield W. Ultrastructural comparison of dissolution and apatite precipitation on hydroxyapatite and silicon-substituted hydroxyapatite in vitro and in vivo. *J Biomed Mater Res A*. 2004;69:670–9.
  35. Wilson CJ, Clegg RE, Leavesley DI, Percy MJ. Mediation of biomaterial-cell interactions by adsorbed proteins: a review. *Tissue Eng*. 2005;11:1–18.
  36. Kokubo T, Kushitani H, Sakka S, Kitsugi T, Yamamuro T. Solutions able to reproduce in vivo surface-structure changes in bioactive glass-ceramic A-W. *J Biomed Mater Res*. 1990;24:721–34.
  37. Jager M, Fischer J, Schultheis A, Lensing-Hohn S, Krauspe R. Extensive H(+) release by bone substitutes affects biocompatibility in vitro testing. *J Biomed Mater Res*. 2006;76:310–22.
  38. Coessens BC, Miller VM, Wood MB. Endothelin-A receptors mediate vascular smooth-muscle response to moderate acidosis in the canine tibial nutrient artery. *J Orthop Res*. 1996;14:818–22.
  39. Li JF, Eastman A. Apoptosis in an interleukin-2 dependent cytotoxic T-lymphocyte cell line is associated with intracellular acidification—role of the  $\text{Na}^+/\text{H}^+$  antiport. *J Biol Chem*. 1995;270:3203–11.
  40. Furlong IJ, Ascaso R, Rivas AL, Collins MK. Intracellular acidification induces apoptosis by stimulating ICE-like protease activity. *J Cell Sci*. 1997;110:653–61.
  41. Suzuki T, Yamamoto T, Toriyama M, Nishizawa K, Yokogawa Y, Mucalo MR, Kawamoto Y, Nagata F, Kameyama T. Surface instability of calcium phosphate ceramics in tissue culture medium and the effect on adhesion and growth of anchorage-dependent animal cells. *J Biomed Mater Res*. 1997;34:507–17.
  42. Hunter GK, Hauschka PV, Poole AR, Rosenberg LC, Goldberg HA. Nucleation and inhibition of hydroxyapatite formation by mineralized tissue proteins. *Biochem J*. 1996;317(Pt 1):59–64.
  43. George A, Veis A. Phosphorylated proteins and control over apatite nucleation, crystal growth, and inhibition. *Chem Rev*. 2008;108:4670–93.
  44. Denhardt DT, Guo X. Osteopontin: a protein with diverse functions. *FASEB J*. 1993;7:1475–82.